

Hopping conductivity in one-dimensional $\text{Ca}_3\text{Co}_2\text{O}_6$ single crystals

B. Raquet,^{1,2} M. N. Baibich,^{1,3} J. M. Broto,^{1,2} H. Rakoto,¹ S. Lambert,⁴ and A. Maignan⁴

¹*Laboratoire National des Champs Magnétiques Pulsés, UMR 5830, 143, Avenue de Rangueil, BP 4245, 31432 Toulouse Cedex 4, France*

²*Laboratoire de Physique de la Matière Condensée, INSA, 135, Avenue de Rangueil, 31077 Toulouse Cedex 4, France*

³*Instituto de Física, UFRGS, Avenida Bento Gonçalves 9500, Caixa Postal 15051, 91501-970 Porto Alegre, RS, Brazil*

⁴*Laboratoire CRISMAT, UMR CNRS 6508, ISMRA, Boulevard du Mal Juin, 14050 Caen Cedex, France*

(Received 20 August 2001; published 4 March 2002)

We studied the electronic conductivity and magnetic properties of quasi-one-dimensional $\text{Ca}_3\text{Co}_2\text{O}_6$ single crystals. The results evidence a variable range hopping conductivity with temperature-induced crossover between one-dimensional (intrachain) and three-dimensional (3D) transport and the opening of a Coulomb gap in the d bands along with the ferromagnetic intrachain ordering. At low temperatures, an applied magnetic field induces a large negative magnetoresistance (MR) in apparent dissociation with the 3D magnetic ordering. Both spin-dependent hopping and field-induced suppression of the Coulomb gap are discussed. The electronic hopping parameters we infer agree remarkably with the accessible Co sites. Surprising narrow peaks corresponding to a transient resistivity decrease are observed on the MR curves. We discuss these in terms of peculiar in-plane magnetization states in an Ising-like Heisenberg antiferromagnetic triangular lattice during the magnetization reversal.

DOI: 10.1103/PhysRevB.65.104442

PACS number(s): 75.10.Dg, 72.20.Ee

I. INTRODUCTION

Over the years, both electronic transport theories and experimental studies have dealt with the problem of charge conduction in low-dimensional systems.¹ Among the metal oxides, the dimensionality usually refers to the metal-metal distances that may be shorter within a plane or along one crystalline direction. The single-crystal growth of low-dimensional oxides provides fascinating experimental model systems to study the interplay between the electronic correlations, the lattice dimensionality, and the resulting electronic conductivity.^{2,3} This paper deals with conduction in a low-dimensional cobalt oxide single crystal that, on account of the peculiarities of the structure, produces an almost perfect realization of a one-dimensional chain of metallic atoms.⁴ The fact that one is dealing with a single crystal, a result of mastering the appropriate technology for crystal growth, enhances the nearly ideal conditions for the experiments performed. A supplementary touch comes from the fact that the metallic chains are constituted by Co, a magnetic ion. We therefore address the question of conductivity of a nearly ideal spin chain where the charge carriers move by occupying states allowed by the magnetic spin state in the alternating Co sites. The fact that these spin chains form a three-dimensional (3D) array, described as an Ising-like Heisenberg triangular net, introduces an extra element to consider: a strong interplay between the “pure” intrachain conduction and the 3D magnetic frustrations is expected to strongly influence the electronic correlations, giving rise to phenomena in the area of low-dimensional conductors.

The $\text{Ca}_3\text{Co}_2\text{O}_6$ compound belongs to the A'_3ABO_6 formula oxides ($A' = \text{Ca}, \text{Sr} \dots$, $A = \text{Ni}, \text{Cu}, \text{Zn} \dots$; $B = \text{Co}, \text{Ir}, \text{Pt} \dots$). It consists of parallel one-dimensional $\text{Co}_2\text{O}_6^{6-}$ chains separated by Ca^{2+} ions.⁵⁻⁷ The chains are built by successive alternating face-sharing CoO_6 trigonal prisms and CoO_6 octahedra along the hexagonal c axis. The resulting

short metal-metal intrachain distance (0.28 nm) compared to the interchain separation (0.524 nm) strongly reinforces the one-dimensional character of the structure along the c axis.⁷ Each Co chain is surrounded by six chains constituting a hexagonal cell in the basal plane. Recent magnetic studies reveal an intrachain ferromagnetic ordering ($T_{c1} \approx 24$ K) and a weaker antiferromagnetic (AF) interchain coupling ($T_{c2} \approx 12$ K).⁸⁻¹² Experimental evidence of a field-induced transition from a ferrimagnetic (Fi, where only two out of three chains are oriented with the field), to a ferromagnetic state (Fo, where all chains follow the field) suggests that $\text{Ca}_3\text{Co}_2\text{O}_6$ behaves as a planar Ising-like Heisenberg AF triangular lattice where each chain acts as a single localized spin.¹⁰⁻¹² The triangular spin lattice with AF coupling induces a partially disordered antiferromagnetic (PDA) state between T_{c1} and T_{c2} and a spin-frozen-like behavior at lower temperatures.¹⁰ The Co spin state on the octahedra and trigonal prisms is still unclear, as discrepancy persists between low-temperature neutron-diffraction analysis and the high-field magnetization values but, from the expected crystal fields, each site should have different moments.⁸ In that respect, at least two different configurations have been sketched for the Co sites:^{8,11} (i) $\text{Co}_{\text{oct}}^{\text{III}}-d^6$, low spin with $\mu \approx 0 \mu_B$ and $\text{Co}_{\text{trig}}^{\text{III}}-d^6$, high spin with $\mu \approx 4 \mu_B$ and (ii) $\text{Co}_{\text{oct}}^{\text{IV}}-d^5$, low spin with $\mu \approx 1 \mu_B$ and $\text{Co}_{\text{trig}}^{\text{II}}-d^7$, high spin with $\mu \approx 3 \mu_B$.

The proposed spin states and the presence of long-range ferromagnetic order along the chains support the idea of partially filled d bands with unpaired electrons on Co sites.³ These electrons are thought to contribute both to electronic conductivity and magnetic ordering. In addition to the unidimensional structure, the eventual d -orbital overlaps between intrachain Co sites,³ the electron-electron interactions, the crystal-field effects on the Co_{oct} and Co_{trig} localized states, and the 3D low-temperature magnetic order may have a severe impact on the conductivity. The $\text{Ca}_3\text{Co}_2\text{O}_6$ compound is

therefore a unique candidate to study electronic transport in low-dimensional frustrated magnetic systems.

We report here unusual electronic transport properties of the $\text{Ca}_3\text{Co}_2\text{O}_6$ single crystal and their apparent association with the inter- and intrachain magnetic ordering, the one-dimensional spin structure, and Coulomb interactions among the valence electrons. The temperature dependence of the conductivity reveals a weak insulator behavior with four temperature regimes from 2 to 450 K. Conduction undergoes a dimensionality crossover from the intrachain (1D) to a 3D variable range hopping (VRH) transport associated with a Coulomb gap opening with energies of the order of 30 K.

Peculiar electronic correlation in the low-dimensional structure is thought to induce the d -band Coulomb gap concomitant with the ferromagnetic ordering within the chains. At low temperatures, an applied magnetic field induces a giant negative magnetoresistance (MR) in apparent dissociation with the 3D magnetic order and the high-field magnetization. From the high-field resistivity vs temperature analysis, we sketch a field-induced suppression of the Coulomb gap responsible for the large decrease in resistivity and we obtain the hopping parameters in the saturated magnetic state in agreement with accessible Co sites. Superimposed on the monotonous and negative MR, remarkably narrow peaks corresponding to transient resistivity reduction are observed on the MR curves. This effect is discussed in terms of specific magnetization states in an Ising-like Heisenberg AF triangular lattice with nonzero in-plane magnetization during the magnetization reversal.

II. EXPERIMENT

Needlelike $\text{Ca}_3\text{Co}_2\text{O}_6$ single crystals were grown by heating a mixture of $\text{Ca}_3\text{Co}_4\text{O}_8$ and K_2CO_3 in a weight ratio of $\frac{1}{7}$, up to 880 °C for 48 h in an aluminum boat in air and then cooling to room temperature at 100 °C h^{-1} . X-ray diffraction and an energy dispersive spectroscopy cationic analysis confirm the rhombohedral structure and the phase stoichiometry. Magnetization and magnetotransport measurements have been performed in a 40-T pulsed magnetic field using the Laboratoire National des Champs Magnetiques Pulsés (Toulouse) facilities. Special care has been taken for the electronic conductivity measurements working both in dc and ac low currents ($< 40\text{ nA}$), within the ohmic regime.

III. RESULTS AND DISCUSSION

In the temperature range of antiferromagnetic interchain interactions, our magnetization measurements exhibit a step-by-step magnetization reversal with a plateau at one-third of the total magnetization ($1.33\mu_B/\text{mol}$ of $\text{Ca}_3\text{Co}_2\text{O}_6$) (Fig. 1). This plateau reveals a magnetic transition from a partially disordered AF coupling between chains toward a field-induced ferrimagnetic state. Higher fields are required to induce a second magnetization jump corresponding to a full ferromagnetic alignment along the field. The sharpness of the magnetic transitions confirms the monocrystalline nature of our samples with the c axis parallel to the applied field. Comparable results are obtained on oriented polycrystalline

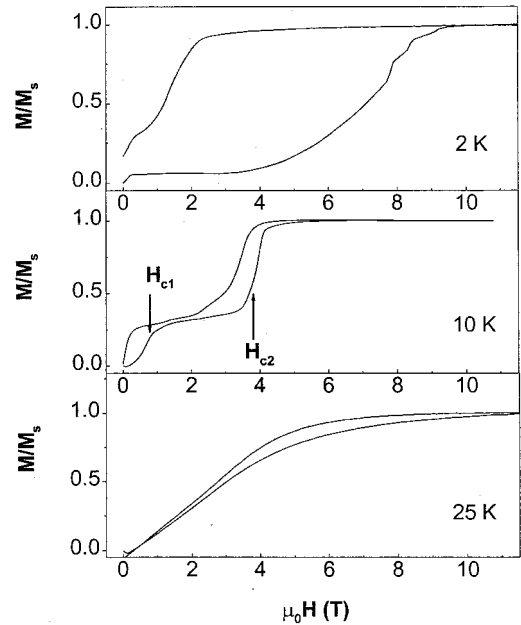


FIG. 1. Magnetization measurements in pulsed field on the $\text{Ca}_3\text{Co}_2\text{O}_6$ single crystal with H parallel to the c axis, at 2, 10, and 25 K.

$\text{Ca}_3\text{Co}_2\text{O}_6$ compounds¹¹ and $\text{Ca}_3\text{Co}_2\text{O}_6$ single crystals.¹² The magnetization measurements in a transversal field (not shown here) support the strong magnetic anisotropy with saturation fields larger than 30 T. The field transitions and the magnetic hysteresis in the longitudinal configuration depend on the temperature and the magnetic-field sweeping rate (5 to 500 T/s) applied during the pulsed field in agreement with dynamic measurements.¹¹ On account of the large sweeping rates, we were not able to reproduce the finer detail of the magnetization at low temperatures observed by Maignan *et al.*¹² on single crystals. The dependence on the sweep rate indicates the predominant role of cooperative effects with slow dynamic processes ($\tau \sim 1\text{ ms}$) that govern the low-temperature magnetization switch within the chains.

Assuming each ferromagnetic chain as a single spin with AF nearest neighbors coupling, the magnetic states are modeled by the molecular-field approximation applied to a Heisenberg AF triangular lattice with uniaxial magnetic anisotropy. Following Miyashita's model,¹³ the experimental values of the critical fields H_{c1} and H_{c2} for the field-induced F_i and F_o states, respectively, give access to the AF interchain coupling J and the chain's anisotropy D . As the magnetic after effects are neglected, the H_{c1} and H_{c2} values are chosen around 10 K for the lowest sweeping rates used, where hysteretic phenomena are small. For an average spin of $1.8\mu_B$ per chain, we infer comparable values for the AF coupling constant $J \approx 3\text{ K}$ and the anisotropy energy along the c axis $D \approx 5\text{ K}$. We point out that the physical origin of the AF interchain interactions remains unclear, as one may expect weak superexchange coupling via the diamagnetic Ca^{2+} ions.

The resistivity, from 2 to 450 K, was measured along the c axis (inset, Fig. 2). Our result extends preliminary measurements, performed by one of us, at higher temperatures.¹²

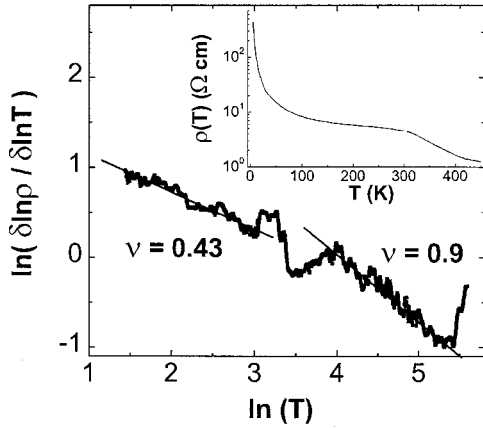


FIG. 2. The log-derivative of the resistivity of the $\text{Ca}_3\text{Co}_2\text{O}_6$ single crystal measured along the chains. The slope of the fit lines equals $-\nu$ (see text). The inset shows the resistivity vs temperature of the $\text{Ca}_3\text{Co}_2\text{O}_6$ single crystal.

A thermally activated behavior is observed over the whole temperature range with a room-temperature resistivity around $4 \Omega \text{ cm}$, far above the metallic limit. The room-temperature resistivity we report is around one order of magnitude smaller than the value previously measured.¹² We attribute this difference to a substantial improvement in the sample's growth toward a grainless structure. The resistivity perpendicular to the chains at 300 K is about 10^4 times larger than the longitudinal one. A small hump on the resistivity curve occurs at 22 K corresponding to the intrachain F_0 temperature, whereas no significant change appears between the PDA phase and the frozen-spin state. We point out that the ferromagnetic ordering within the chains does not induce a conductivity change toward increased metallicity, as is usually observed in transition-metal oxides.¹⁴ Double exchange along the Co-O-Co chains is therefore considered unlikely. The resistivity at low temperatures suggests a strong localization regime with a thermally activated conductivity of the form

$$\rho(T) = \rho_0 \exp\left(\frac{T_0}{T}\right)^\nu. \quad (1)$$

Fractional values of ν , between $\frac{1}{4}$ and 1, refer to variable range hopping (VRH) conductivity:^{15,16} the ν exponent depends on the dimensionality and the eventual existence of electron-electron interactions that would cause a smooth depletion of the density of states at the Fermi energy level (E_F).

We use the well-known logarithmic-derivative technique for an accurate estimate of the ν exponent and the T_0 value. Such analysis is especially adapted for reduced temperature ranges.¹⁷ In Fig. 2 we plot $\ln\{-\partial(\ln \rho)/\partial(\ln T)\}$ vs $\ln T$, where the slopes of the fit give $-\nu$. Four conductivity regimes are unambiguously defined: below 25 K, the resistivity is well described by Eq. (1) with $\nu \approx 0.43$ and $T_0 \approx 600$ K. A temperature-induced transition (crossover) occurs between 30 and 70 K, where the resistivity closely follows $\rho \propto 1/T$. This transition regime is clearly visible on the logarithmic-derivative curve: two very distinct slopes are ob-

served on either side of this transition. From 70 to 230 K, $\rho(T)$ is thermally activated with $\nu \approx 0.9$ and $T_0 \approx 87$ K. This intermediate-temperature regime is limited by a drastic resistivity drop above 230 K, which seems to saturate around 450 K. Let us mention that no hysteretic behavior has been observed in the vicinity of the temperature-induced transitions, and similar $R(T)$ curves are obtained varying the current density through the samples and for different temperature sweeps.

For the low-temperature regime, below 25 K, a hopping exponent about 0.5 is consistent with the Efros-Shklovskii (ES), conductivity-type VRH, i.e., a VRH with a soft Coulomb gap Δ_c due to Coulomb interactions between the localized electrons.¹⁸ Little departure from $\nu \approx 0.5$ usually originates from a nonparabolic gap at E_F .¹⁶ The Coulomb gap is defined by¹⁸ $\Delta_c \approx e^3 N_3(E_F)^{1/2} / \epsilon_0^{3/2} \epsilon_r^{3/2}$. Unfortunately, the permittivity ϵ_r and the 3D electronic density of states at the Fermi level [$N_3(E_F)$] are, to our best knowledge, not yet known for $\text{Ca}_3\text{Co}_2\text{O}_6$, and assumptions of their values would be dangerously speculative. Nevertheless, Coulomb gaps in d valence bands are customarily obtained from the upper temperature limit of the ES regime; we estimate $\Delta_c \approx 30 \pm 10$ K. This gap is thought to drive the hopping energy below 30 K and appears simultaneously with the intrachain ferromagnetic state. The theoretical expressions for the localization length α^{-1} and the average hopping distance $R_{\text{opt}}(T)$ cannot be inferred from straightforward application of the ES model: at low temperatures the antiferromagnetic coupling J between chains induces an additional spin-dependent energy to the electronic hopping energy between interchain sites of opposite spin.

Above the low-temperature transition, from 70 to 230 K, the activated behavior ($\nu \approx 1$) of the conductivity may be associated with different electronic transport mechanisms involving either extended or localized cobalt d states. For instance, activation to a mobility edge¹⁹ or nearest-neighbor hopping²⁰ are possible sources for an activated T^{-1} law. According to the Co-Co distances, a nearest-neighbor hopping hints of an intrachain conductivity with very weakly probable transition rates perpendicular to the chains. The hopping charge carriers successively alternate from the Co_{oct} to Co_{trig} sites and the 87-K activation energy would be related to average energy barriers between the two sites induced by different crystal fields. On the other hand, extended calculations of the variable range hopping process in one-dimensional systems also exhibit an activated T^{-1} law for the conductivity,²¹ irrespective of the asymptotic form of the Mott model.²² If we sketch a 1D-VRH mechanism between 70 and 230 K, the energy gap ΔE is related to the localization length α^{-1} and the density of states $N_1(E_F)$ per unit chain length as $\Delta E \approx k_B T_0 \approx 1/(2N_1(E_F)\alpha^{-1})$, and the average hopping distance is given by $R_{\text{opt}}(T) \approx 2\alpha^{-1}(T_0/T)^{1/2}$.^{21,23} From $\Delta E \approx 87$ K, we infer the ratio between the average hopping distance and the localization $R_{\text{opt}}(T)/\alpha^{-1} \approx 18/\sqrt{T}$, which is always greater than 1, as required for consistency within the temperature range where the thermally activated regime is measured (ratios of ~ 1.3 at 200 K and 2 at 80 K). We also deduce $N_1(E_F) \times \alpha^{-1}$

$\approx 60 \text{ eV}^{-1}$. We underline that the 1D electronic conductivity assumption above 70 K holds if the optimum hopping distance we estimate remains lower than the interchain distance. The condition $R_{\text{opt}}(70 \text{ K}) \approx 2.1 \alpha^{-1} \leq 0.53 \text{ nm}$ implies a localization length of the order of 0.25 nm, which is favorably compared to the Co-Co distance within the chains. From the above condition, we estimate the 1D density of states as $N_1(E_F) \approx 2.5 \times 10^{11} \text{ eV}^{-1} \text{ m}^{-1}$. Such a high value is consistent with extended Hückel calculations on $A_3'ABO_6$ chains, which predict narrow bandwidths for the Co d bands ($W < 0.5 \text{ eV}$) (Ref. 3) and a Fermi level close to maximum. From the number of accessible states in the d band, the interatomic distance, and the calculated bandwidth, we expect $N_1(E_F)$ to be larger than $10^{11} \text{ eV}^{-1} \text{ m}^{-1}$, in good agreement with the value deduced from the 1D-VRH assumption above.

The high-temperature regime, beyond 230 K, represents a departure towards a more conducting regime with saturation expected not too far above 450 K. A close analogy is observed with theoretical predictions for hopping conductivity of quasi-one-dimensional systems composed of weakly coupled 1D filaments:²³ above a critical temperature T^* , the interchain transition rate is significantly increased as the corresponding energies become accessible by phonon-assisted hopping. The temperature T^* is related to the VRH parameters and the interchain distance d by²³

$$T^* \approx \sqrt{\frac{d}{\alpha^{-1}}} \frac{1}{k_B \alpha^{-1} N_1(E_F)}. \quad (2)$$

According to the VRH parameters defined above, Eq. (2) yields an estimated crossover temperature of the order of $T^* \approx 250 \text{ K}$, very close to the experimental temperature limit we measure for the thermally activated regime. We interpret the high-temperature plunge of the resistivity about T^* as a second electronic dimensionality change from a 1D transport along the chains to a more conducting 3D regime. The consistency of the hopping parameters we extract and the experimental evidence of the temperature crossover T^* tend to confirm the variable range hopping mechanism along the one-dimensional chains in the intermediate-temperature regime. And we speculate that, above T^* , the interchain electronic hopping contributes to the optimal electronic path avoiding low transition rates within the chains due to local defects.

Application of a magnetic field should reveal, in terms of conductivity, the role of spin ordering in these systems. The longitudinal high-field magnetoresistance measurements show a negligible field effect on the resistivity above 25 K, as the system is paramagnetic in this temperature range. However, below the ferromagnetic ordering temperature, a negative MR appears that drastically increases with decreasing temperature, reaching around 80% at 2 K [Fig. 3(a)]. At the lowest temperatures explored, the large MR exhibits a strong decrease in low fields (below $\approx 7 \text{ T}$). Above 10 K, $\rho(H)$ continuously decreases with no hints of saturation for higher fields.

On the $\rho(H)$ curve plotted for both the increasing and decreasing pulsed field [Fig. 3(b)], we point out two very deep minima corresponding to “transient” resistivity de-

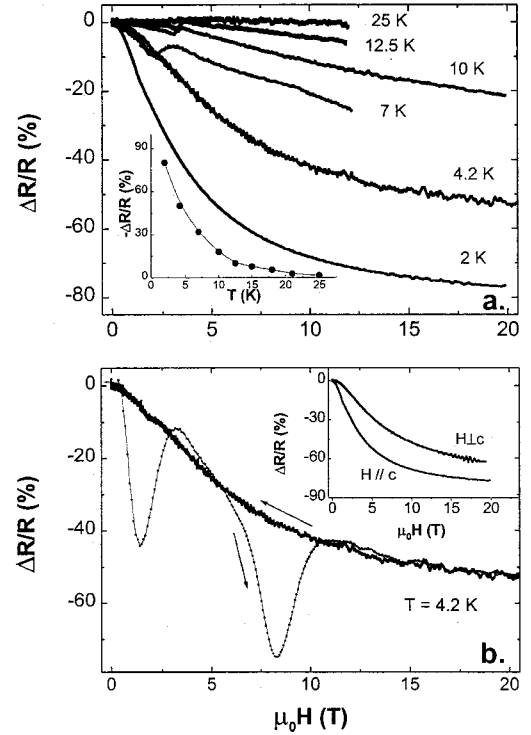


FIG. 3. (a) Magnetoresistance in pulsed field of the $\text{Ca}_3\text{Co}_2\text{O}_6$ single crystal in the longitudinal configuration, $i//H//c$ axis for various temperatures. Only the MR curves for the decreasing field are plotted. The inset shows the $\Delta R/R(\%)$ at 20 T as a function of the temperature. (b) Complete plot of the MR curves at 4.2 K for the increasing and decreasing pulsed field. One notices that the transient resistivity decreases during the increase of the field. The inset shows the MR anisotropy at 2 K for $H//c$ axis and H perpendicular to the chains.

creases. They are superimposed on the monotonous and reversible $\rho(H)$ decrease. The peaks appear at critical fields both depending on the temperature and the field dynamics; $H_{c1} \approx 2$ and $H_{c2} \approx 7 \text{ T}$ at 10 K, and those values continuously increase by 30% for a sweeping rate varying from 100 to 250 T s^{-1} . We point out that the magnitude of the first peak occurring at H_{c1} is strongly magnetic history dependent. The second one is, however, systematically reproduced whatever the thermal cycling and previous applied fields. Such astonishing singularities are only visible on the longitudinal configuration. When the field goes back to zero at a much lower sweeping rate, only a small dip is observed around 2.5 T; it also corresponds to a transient resistivity decrease. It is worth mentioning that the MR anisotropy reveals a relatively small difference in magnitude and saturation field between the longitudinal and transverse configurations, unlike the magnetization [inset, Fig. 3(b)]. The present results suggest both field-induced effects on the electronic structure and eventual correlations between the magnetic states and electronic conductivity, i.e., spin-dependent transport on Co sites.

Direct comparison of the MR(H) curves and the magnetization obtained for identical pulsed field configurations are of great interest [Figs. 4(a) and 4(b)]. First, the monotonous resistivity decrease we observe seems uncorrelated to the step-by-step magnetization process. For instance, at 4 K (Fig.

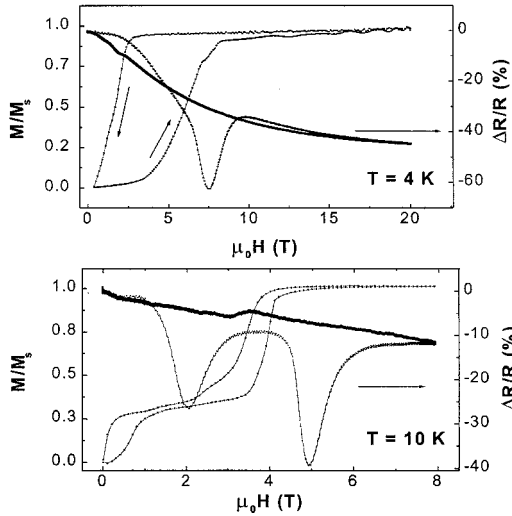


FIG. 4. Magnetization and magnetoresistance of the $\text{Ca}_3\text{Co}_2\text{O}_6$ single crystal in the longitudinal configuration at 4 (top panel) and 10 K (bottom panel).

4, top panel), starting from the high-field saturated state, the magnetization remains constant for a decreasing field down to 2.5 T whereas, in the same field range, the MR continuously varies from 45% to 8%. The full magnetization jump at 2.5 T towards the zero-field value only induces a tiny resistivity change. The same behavior holds for higher temperatures. Also, the weak MR anisotropy compared to that observed for magnetization further shows that the large magnetoresistance below 20 K is not correlated to the 3D magnetic ordering. However, it turns out that the transient resistivity decrease seems closely connected to the field-induced magnetic transitions during the magnetization process.

Theoretical simulations of the magnetization for an Ising-like Heisenberg AF triangular lattice have shown the appearance of a transient in-plane component of the magnetization when it is reversed from the Fi to the Fo state along the easy axis.¹³ A possible explanation for the conductivity peaks may be an electronic coupling with a peculiar state of the magnetization when the AF coupling between chains is broken by a longitudinal field. The interchain electronic hopping that contributes to a conductivity enhancement may then be favored by the existence of a nontrivial component of the magnetization perpendicular to the chains. On the other hand, the dependence on the field dynamics suggests that the internal magnetic-flux variations during the magnetization jumps may also be responsible for induced voltages related to dM/dt and superimposed on the monotonous MR signal.²⁴ However, we systematically measure a transient decreasing voltage that roughly scales with the applied current. Even if this tends to confirm the role of induced voltages, more experiments are required, particularly in static fields.

The high-field resistivity $\rho_{(H=15\text{ T})}(T)$, well above the technical saturation of the magnetization, i.e., in the interchain Fo state, still exhibits a weak insulating behavior. The plot of $\ln[\rho_{(H=15\text{ T})}(T)]$ versus $1/T^{1/4}$ shows a much better linear dependence than that obtained using the zero-field ν exponent (Fig. 5). This strongly suggests a field-induced

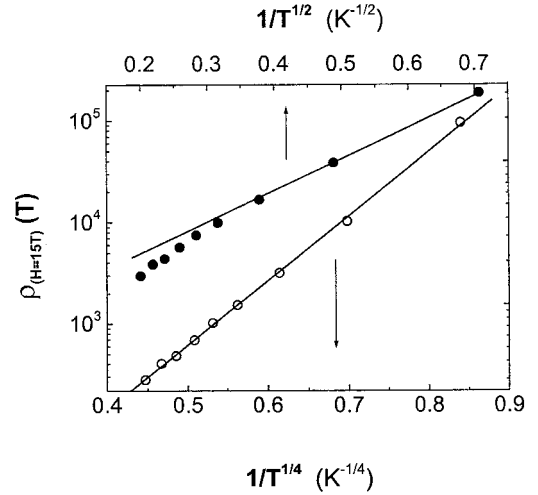


FIG. 5. High-field resistivity at 15 T, $\rho_{(H=15\text{ T})}(T)$, vs $T^{-1/2}$ (top scale) and $T^{-1/4}$ (bottom scale). Solid lines are the best linear fits.

transition from the ES conductivity to a 3D-Mott VRH regime²² in the saturated magnetic state. This means that the Coulomb gap in the d bands we observe in zero field, below 30 K, is drastically reduced by the applied field. This is not surprising as the Zeeman energy at 15 T is comparable to the Coulomb gap for a Landé factor of 3.7.¹¹ From the linear fit of $\ln[\rho_{(H=15\text{ T})}(T)]$ versus $1/T^{1/4}$, we deduce $T_0 \approx 11\,500$ K. In the frame of the standard 3D-Mott model, the localization length is defined by $\alpha^{-1} \approx 18/\{kT_0 N_3(E_F)\}^{1/3}$ and the average hopping distance is²²

$$R_{\text{opt}}(T) = \{9/(8\pi N_3(E_F)kT)\}^{1/4}.$$

Assuming a temperature-independent density of states, the 3D density $N_3(E_F)$ should be related to the one-dimensional $N_1(E_F)$ along the chains by $N_3(E_F) \approx N_1(E_F)/d^2$, where d is the interchain Co-Co distance. From the estimated $N_1(E_F)$ value in the intermediate-temperature regime, we get $N_3(E_F) \approx 6 \times 10^{29} \text{ eV}^{-1} \text{ m}^{-3}$. So, below 25 K and in the saturated magnetic state, we infer $\alpha^{-1} \approx 0.28$ and $R_{\text{opt}}(T) = 1.3/T^{1/4} \text{ nm}$. The localization length remains comparable to that obtained above 70 K close to the metal-metal intrachain distance, and the average hopping distance is large enough for electronic hopping between nearest and next-nearest chains below 25 K (0.6 nm at 20 K and 0.9 nm at 4 K).

IV. CONCLUDING REMARKS

The conductivity analysis evidences two temperature-induced electronic dimensionality crossovers. In the intermediate-temperature regime, between 70 and 230 K, we interpret the activated T^{-1} law as VRH within the chains with a localization length of the order of the metal-metal distance and a rather high density of states at E_F . For higher temperatures, the resistivity drop we observe strongly suggests a transition toward a 3D regime for which the required interchain transition energies become accessible by phonon-assisted hopping. When the temperature is lowered below the ferromagnetic ordering T_{c1} , the VRH mechanism exhibits

two changes taking place in the transition temperature range: on one hand, the increase of the average hops above the interchain distance below 70 K induces a crossover from 1D to 3D hopping. Despite the one-dimensional structure of the Co chains, the effective dimensionality of the VRH state is 3D. On the other hand, the opening of a correlation gap at E_F within the d bands drives the hopping energies between sites and consistently explains the $T^{1/2}$ law below 30 K. The appearance of a Coulomb gap along with the intrachain ferromagnetic interaction is a puzzling phenomenon, which, to our best knowledge, remains to be explored.²⁵ The effect of a magnetic field on the conductivity clearly evidences a field-induced Coulomb gap reduction responsible for the large resistivity decrease. The discrepancy between the magnetization curves and the magnetoresistance behavior suggests that the VRH process is essentially governed by the magnitude of

the Coulomb gap. We support the idea that the influence of the low-temperature 3D magnetic ordering including the PDA and the frozen-spin states on the spin-dependent hops is not determinant. Among the accessible nearest and next-nearest Co sites, both parallel and antiparallel magnetic ions exist in the fundamental magnetic ground states.¹² Finally, superimposed on the magnetoresistance, the deep resistivity minima we measure at certain fields are probably related to peculiar transient perpendicular states of the frustrated triangular lattice during the magnetization reversal. They may evidence a nontrivial spin-orbit coupling that drives the interchain hopping rates. More investigation is required to clarify the existence of a Coulomb gap in a low-dimensional ferromagnetic structure as well as the spin-dependent hopping mechanisms between the trigonal and octahedral sites.

-
- ¹P. W. Anderson, *Phys. Today* **50** (10), 42 (1997).
²T. N. Nguyen and H.-C. zur Loye, *J. Solid State Chem.* **117**, 300 (1995).
³G. V. Vajenine, R. Hoffmann, and H.-C. zur Loye, *Chem. Phys.* **204**, 469 (1996).
⁴K. Yamaura, H. W. Zandbergen, K. Abe, and R. J. Cava, *J. Solid State Chem.* **146**, 96 (1999).
⁵C. Brisi and R. Rolando, *Ann. Chim. (Rome)* **58**, 676 (1968).
⁶E. Woermann and A. Muan, *J. Inorg. Nucl. Chem.* **32**, 1455 (1970).
⁷H. Fjellvag, E. Gulbrandsen, S. Aasland, A. Olsen, and B. C. Hauback, *J. Solid State Chem.* **124**, 190 (1996).
⁸S. Aasland, H. Fjellvag, and B. Hauback, *Solid State Commun.* **101**, 187 (1997).
⁹B. Martinez, V. Laukhin, M. Hernando, J. Fontcuberta, M. Parras, and J. M. Gonzalez-Calbert, *Phys. Rev. B* **64**, 012417 (2001).
¹⁰H. Kageyama, K. Yoshimura, K. Kosuge, H. Mitamura, and T. Goto, *J. Phys. Soc. Jpn.* **66**, 1607 (1997).
¹¹H. Kageyama, K. Yoshimura, K. Kosuge, M. Azuma, M. Takano, H. Mitamura, and T. Goto, *J. Phys. Soc. Jpn.* **66**, 3996 (1997).
¹²A. Maignan, C. Michel, A. C. Masset, C. Martin, and B. Raveau, *Eur. Phys. J. B* **15**, 657 (2000).
¹³S. Miyashita, *J. Phys. Soc. Jpn.* **55**, 3605 (1986).
¹⁴M. Coey, M. Viret, and S. von Molnar, *Adv. Phys.* **48**, 167 (1999).
¹⁵A. G. Zabrodkii and K. N. Zino'eva, *Sov. Phys. JETP* **59**, 425 (1984).
¹⁶M. E. Raikh and I. M. Ruzin, *Sov. Phys. JETP* **68**, 642 (1989).
¹⁷A. Hunt, *Solid State Commun.* **86**, 765 (1993).
¹⁸A. L. Efros and B. Shklovskii, *J. Phys. C* **8**, L49 (1975).
¹⁹M. Cluster and N. F. Mott, *Phys. Rev.* **181**, 1336 (1969).
²⁰O. Madelung, in *Introduction to Solid-State Theory*, edited by M. Cardona, P. Fulde, and H.-J. Queisser (Springer-Verlag, Berlin, 1978).
²¹J. Kurkijärvi, *Phys. Rev. B* **8**, 922 (1973).
²²N. F. Mott, *J. Non-Cryst. Solids* **1**, 1 (1968).
²³I. P. Zvyagin, *JETP* **80**, 93 (1995).
²⁴M. Viret (private communication).
²⁵K. Yamaura, D. P. Young, and R. J. Cava, *Phys. Rev. B* **63**, 064401 (2001).